CrossMark

Thermal analysis in foundry technology

Part 2. TG–DTG–DSC, TG–MS and TG–IR study of the new class of polymer binders BioCo

Beata Grabowska[1] · Krzysztof Hodor[2] · Karolina Kaczmarska[1] · Artur Bobrowski[1] ·
Żaneta Kurleto-Kozioł[1] · Carolin Fischer[3]

Abstract In this study, a polymer composition of poly (acrylic acid) and dextrin (PAA/D) cross-linked with microwave radiation, belonging to the new BioCo group of environmentally friendly foundry binders, was subjected to thermal analysis (TG–DTG–DSC, TG–MS, TG–IR) in a temperature range of 20–600 °C. A thermal analysis of PAA/D compositions enables the determination of a temperature range at which the composition is not susceptible to thermal degradation and thus does not lose its binding properties. The study showed that the process of thermal degradation of PAA/D is complex and multi-stage (TG–DTG–DSC). Within a temperature range of 20–250 °C, physical and chemical changes take place associated with the evaporation of the water fraction of the solvent (20–100 °C), next with the evaporation of the water hydration and finally with intermolecular dehydration reactions (100–250 °C). Above a temperature of 300 °C, the decomposition of the polymer chains takes places, and thereafter, the intensive degradation of PAA/D occurs together the creation of gaseous substances, primarily low molecular weight inorganic (CO_2, H_2O, CO) and organic compounds, including methane (TG–IR, TG–MS).

✉ Beata Grabowska
  beata.grabowska@agh.edu.pl

1   Faculty of Foundry Engineering, AGH - University of
    Science and Technology, Reymonta 23, 30 059 Krakow,
    Poland

2   Netzsch Instrumenty Sp. zo.o., ul. Halicka 9, 31-036 Kraków,
    Poland

3   NETZSCH-Gerätebau GmbH BU Analyzing and Testing,
    Selb, Germany

Introduction

The polymer materials, solvents and organic hardeners used in foundry sands are the main source of hazardous compounds emitted by these sands. Emissions of such compounds may begin to take place as early as the mass preparation stage, when volatile organic substances, mainly solvents, are released. The majority of these gaseous substances, however, arise when the sand comes into contact with the molten metal, as high temperatures lead to thermal degradation of their organic components [1–3].

The level of gas emissions from foundry sands becomes relevant in the context of maintaining workplace safety at the foundry, as well as having an influence on the final quality of the cast. Techniques which make use of organic components containing phenyls, amines and sulphurs are potentially harmful. The impact of the amines released during the hardening of the sand, and of aromatic hydrocarbons generated during the degradation of the organic mass is not neutral for environment [4–6]. Moreover, the technological and economic aspects must be taken into consideration, as the gasses released during degradation (including SO_2) may enter into undesirable reactions at the mould–foundry sand interface, leading to significant casting flaws, including deterioration of the state of the cast's surface [7, 8]. Foundry sands containing polymer BioCo binders are characterised by satisfactory mechanical durability after hardening [9]. The use of these new BioCo binders in the form of polymer compositions in the foundry sands ensures that a mould for casting iron can be achieved which meets the requirements both in terms of quality and

of durability for the selected type of iron, while also creating a cast which does not present difficulties during removal from the mould. The casts are free of flaws, and the results of durability tests conducted on samples of casts confirm that ductile cast iron is obtained. BioCo binders in the form of aqueous compositions of poly(acrylic acid) polymers and modified polysaccharide (dextrin, carboxymethyl starch) are environmentally friendly binding materials (for sand grains SiO_2). These materials include polymer compositions of poly(acrylic acid) and dextrin (PAA/D). BioCo binders do not contain harmful substances and are soluble in water. It has been proven that in the field of microwave radiation under via adsorption goes the transient formation of networks as result of hydrogen bonds. Hydrogen bonds are mainly responsible for upholding cross-linked structures in the system binder–sand grains. Under the influence of microwave radiation at increased temperatures, the cross-linking reaction occurs by the PAA dehydration and anhydride bonds are formed (Fig. 1) [10, 11].

The benzene, toluene, ethylbenzene and xylenes (BTEX) emission levels which take place when the molten cast iron is poured into the mould of foundry sands containing BioCo binder remain low, as indicated by experimental analysis conducted in semi-technical conditions [9].

However, in order to fully understand the process of occurrence of gaseous substances when the molten metal comes into contact with the mould, it is essential to understand the degradation process of the binder itself. It can be assumed that the thermal degradation process of the binder takes place in anaerobic conditions, although in moulds of a non-homogeneous structure a certain amount

of trapped air may be found. Additionally, the interior of the mould into which the molten metal is poured is filled with air. Therefore, the thermal degradation of the binder takes place with the limited participation of oxygen, and the mechanism for the degradation reaction may be considered to be mixed [4, 12, 13]. Moreover, at a distance of 5–30 mm from the cast–mould interface, a temperature of between 300 and 600 °C is maintained for approximately 1 h. This temperature range may be conducive to many reactions, mainly to degradation, including cyclisation and dehydrogenation [12]. Moreover, the dynamic process of the emission of gaseous products of degradation and their increased pressure on the mould may also cause localised increases in pressure which are conducive to degradation reactions. In such conditions, low molecular weight compounds arising from partial degradation and also alkyl radicals undergo further changes. These reactions may thus lead to the occurrence of hydrocarbons, including aromatic hydrocarbons [14].

There are several methods of measurement related to qualitative and quantitative analysis of gasses emitted during the process of pouring molten metal into the mould [15]. Some of these methods permit the amount and kinetics of the gasses emitted to be determined and allow for the analysis of aromatic hydrocarbons, including benzene, toluene, ethylbenzene and xylenes (BTEX), released when the molten metal is poured into the mould [2]. During this pouring process, gaseous substances are released from the mould and conducted through the discharge system, next through the drying system and finally onto an adsorber (activated carbon) where the adsorption of the organic compounds contained in the gasses flowing through the

Fig. 1 Cross-linking hydrogen bonds in the binder–sand grains system [10]
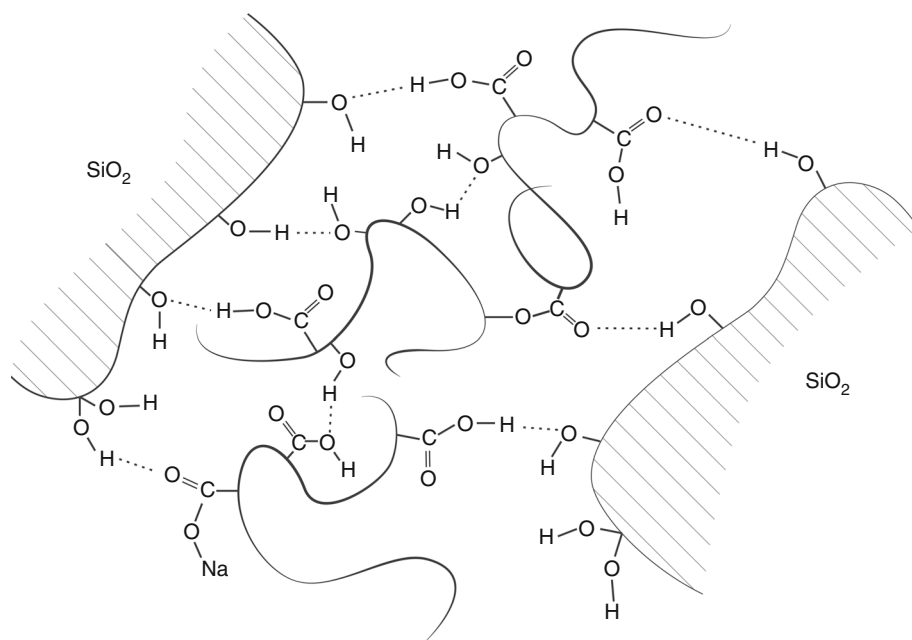
system takes place [16]. This adsorption takes place successively in two separate layers, a measuring layer and a control layer. The control layer serves to capture those gasses which were not adsorbed by the first measuring layer. The gasses which are adsorbed by the activated carbon of the measuring and control layers, after any carbon disulphide (CS_2) has been extracted, are subjected to analysis by gas chromatography (GC) using a flame ionisation detector (FID).

In this study, an analysis of the thermal degradation process of polymer binders in the form of a composition of PAA/D was conducted, based on the literature regarding the degradation of polyacrylic acid polymers and polysaccharides, as well as on the results of the authors' own research (TG–DSC, TG–MS, TG–IR) [3, 17–21]. To determine the values of degradation temperatures and the thermal effects which took place during heating of composition samples, TG and DSC thermal analysis (TA) methods were used. The results of TG–DSC analysis for polymer compositions containing poly(acrylic acid) and polysaccharides have already been presented in the first part of this publication [13]. In this work, an attempt was made to identify the thermal degradation process of the PAA/D polymer composition based on extended TG–DTG–DSC thermal analysis, taking into consideration volatile products of degradation using two coupled techniques; TG–MS—thermogravimetry directly coupled to mass spectrometry and TG–IR—thermogravimetry online coupled to Fourier transform infrared spectroscopy (FTIR). The data obtained are also crucial in regard to the optimisation of conditions for cross-linking with microwave radiation and for conventional heating methods for the PAA/D composition, as well as in the context of the processes taking place in the cast–mould complex associated with the emission of gaseous products and their impact on the quality of the cast.

Experimental

Material

Thermal analysis involved polymer composition of PAA/D cross-linked with microwave radiation. Their characterisation and cross-linking condition PAA/D are provided in Table 1.

Thermal examinations

The NETZSCH model STA 449 *F3 Jupiter*® simultaneous thermal analyser can be used to measure the mass change and transformation energetics of a wide range of materials. The top-loading STA can be equipped with

Table 1 Characteristics of compositions and their cross-linking parameters

Polymer	Composition	Hardening conditions
PAA/D	62% aqueous solution of poly(acrylic acid) (PAA, 100,000 g mol^{-1}, BASF) and dextrin (D, modified potato starch, Fluka), in a mass ratio 7:8, pH 1.5	Microwave device: RM 2001 Pc, Plazmatronica Microwave power of 800 W Frequency of 2.45 GHz Microwave action time: 60 s Temperature inside the device: 100 °C

various easily exchangeable TG, TG–DTA or true TG–DSC sensors and with different furnaces to accommodate different temperature ranges. The system employed for this work was equipped with a silicon carbide furnace capable of operation from room temperature to 1550 °C. The system is vacuum tight, allowing measurements to be conducted under pure inert, reducing or oxidising atmospheres. Heating rates of up to 50 K min^{-1} can be employed and the digital resolution of the balance is 1 µg digit^{-1}. Data acquisition and evaluation, as well as instrument control, are carried out using an MS-Windows software package. The software allows the computation of the rate of mass change, mass change steps, onset and peak temperatures, inflection points and peak area integration.

The Thermo-Microbalance NETZSCH TG 209 *F1 Iris*® with an effective resolution of 0.1 µg enables highly precise measurements under pure gas atmospheres from ambient temperatures up to 600 °C. Internal mass flow controllers (MFC) guarantee a highly precise gas flow adjustment of three different gases.

Data exchange between NETZSCH *PROTEUS* software and Bruker *OPUS* software is done online during the measurement. This guarantees simultaneous start and stop of the measurement as well as data exchange during the measurements.

The IR system is a commercial system of the company Bruker (Tensor 27) with a special external gas cell for TG coupling (TG–IR, also available from Bruker). The TG–IR extension is equipped with a separated MCT detector and a gas cell with an optical path length of 123 mm and an internal volume of 8.7 mL. The transfer time between TG and IR is dependent of the selected gas flow of the TG and covers typically a range of about 15–20 s. However, this time offset is automatically corrected during the evaluation of the TG–FTIR data.

Table 2 Measurement parameters

Parameters	STA-MS	TG–IR
Temperature program	40–600 °C	RT—600 °C
Heating rate	20 K min^{-1}	20 K min^{-1}
Atmosphere	Nitrogen	Nitrogen
Flow rate	70 mL min^{-1}	40 mL min^{-1}
Sample holder	TG–DSC type S	sample carrier for corrosive gases
Crucible	Platinum with pierced lids	Al$_2$O$_3$ (85 μL)
Sample mass	10.50 mg	24.43 mg

Table 2 presents the collected STA-MS and TG–IR measurement parameters.

Results and discussion

The results of TG–DSC analysis (in oxygen and oxygen-free atmosphere) for polymer compositions containing poly(acrylic acid) and polysaccharides (polymer binders BioCo) have already been presented in the first part of this publication [13]. In this work (Part 2), an attempt was made to identify the thermal degradation process of the PAA/D polymer composition based on extended TG–DTG–DSC thermal analysis, taking into consideration volatile products of degradation using two coupled techniques; TG–MS—thermogravimetry directly coupled to mass spectrometry and TG–IR—thermogravimetry online coupled to Fourier transform infrared spectroscopy (FTIR). The thermal degradation of the binder in the mould takes place with the limited participation of oxygen (conditions
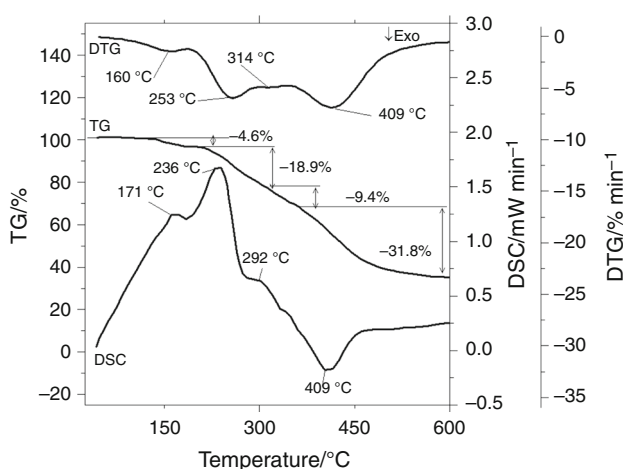
corresponding to the process of pouring the liquid metal/alloy into a mould). Therefore, this paper presents thermal analysis in oxygen-free conditions.

Figure 2 depicts the temperature-dependent mass change (TG), rate of mass change (DTG) and heat flow rate (DSC) of the polymer mixture PAA/D. In total, four mass loss steps of 4.6, 18.9, 9.4 and 31.8% were observed. The maximal mass loss rates were observed at the temperatures 156, 257, 314 and 409 °C which can be seen from the DTG signal. In correlation with the mass loss steps, different energetic effects occurred in the DSC signal. Three overlapping endothermic effects with peak temperatures of 171, 236 and 292 °C occurred. The fourth mass loss step correlated with an exothermic peak at 409 °C. The PAA/D degradation mechanism included dehydration, the formation of anhydride-type structures and their decarboxylation, chains scission and depolymerisation. Physically absorbed water was released during the first stage with a small mass loss. The next stages involved anhydride formation and decarboxylation. The last stage during the pyrolysis of PAA/D probably was associated with the release of acrylic acid (depolymerisation), decomposition of polymer chains (poly(acrylic acid), dextrin), or oxidation process of the partially decomposed matter in a wide temperature range, from 400 to 600 °C. Above 400 °C in nitrogen atmosphere, a carbonaceous residue was generated (a residual mass of 35.3%) [13, 21, 22].

Information obtained by analysing the TG–DSC curves for the PAA/D composition is presented in Table 3.

Figure 3 presents the most intensive mass numbers as a result of mass spectrometry for PAA/D. The mass numbers 15, 16, 17 and 18 showed significant intensity up to 450 °C and mass number 15 has an additional maximum at 530 °C. Mass numbers 17 and 18 are probably due to the release of radical $^*OH$ and moisture (H_2O). The mass numbers 15 and 16 could be due to radical $^*CH_3$ and methane (CH_4). These evolved gases correlate with the mass loss steps three and four.

Figure 4 depicts the mass numbers 41, 42, 43 and 44 which were released between 250 and 550 °C and are

Fig. 2 TG–DTG–DSC curves of PAA/D composition

Table 3 Analysis of TG–DSC curves of PAA/D composition in a nitrogen atmosphere

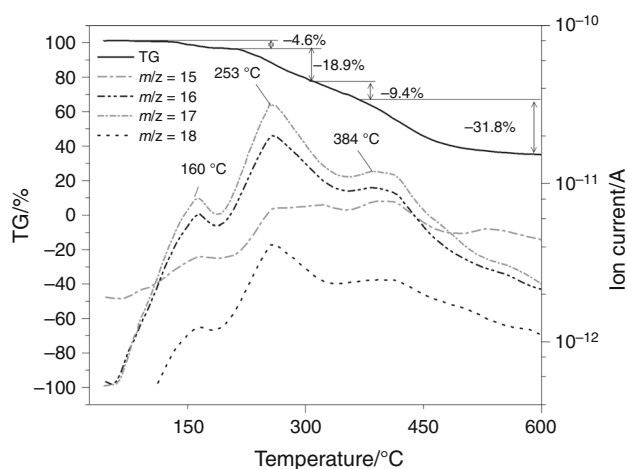| Stage	Oxygen-free atmosphere		
I	Δm/%	Temp. of maximum rate of mass loss/°C	DSC effect temperature/°C
II	4.6	156	endo-171
III	18.9	257	endo-236
IV	9.4	314	endo-292
	31.8	409	exo-409
	Remaining sample mass 35.3%		

Fig. 3 Temperature-dependent mass change (TG–MS) results of mass spectrometry, ion current for mass numbers: 15 (line $m/z = 15$), 16 (line $m/z = 16$), 17 (line $m/z = 17$) and 18 (line $m/z = 18$) of PAA/D composition
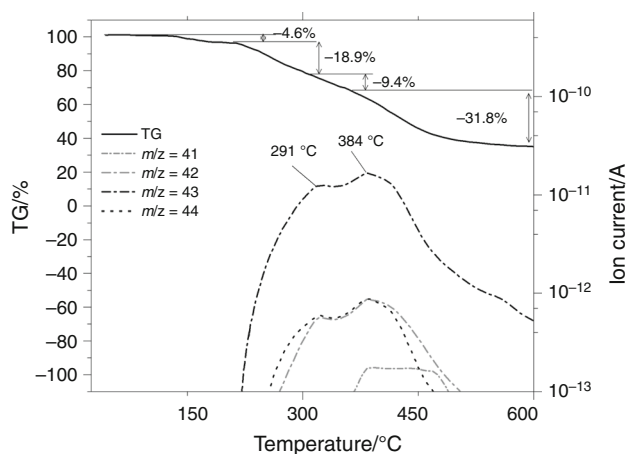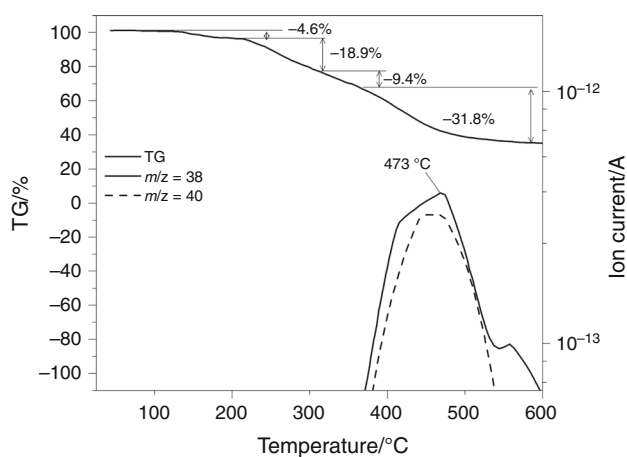

Fig. 4 Temperature-dependent mass change (TG–MS) results of mass spectrometry, ion current for mass numbers: 41 (line $m/z = 41$), 42 (line $m/z = 42$), 43 (line $m/z = 43$) and 44 (line $m/z = 44$) of PAA/D composition

Fig. 5 Temperature-dependent mass change (TG–MS) results of mass spectrometry, ion current for mass numbers: 38 (line $m/z = 38$) and 40 (line $m/z = 40$) of PAA/D composition
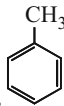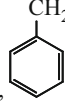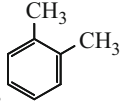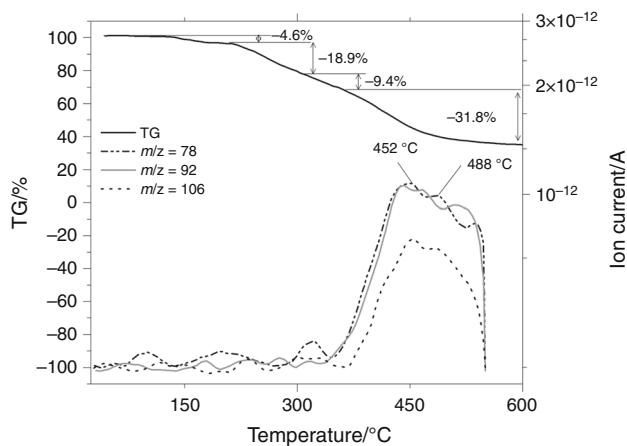

Fig. 6 Temperature-dependent mass change (TG–MS) results of mass spectrometry, ion current for mass numbers: 78 (line $m/z = 78$), 92 (line $m/z = 92$) and 106 (line $m/z = 106$) of PAA/D composition

associated with the mass loss steps three and four. Mass number 44 may be identified as carbon dioxide (CO_2) and 42—propene (C_3H_6). The comparison to the NIST Atomic Spectra Database revealed that at 384 °C propene may be released [23].

The release of the mass numbers 38 and 40 mainly occurred between 350 and 550 °C and is related to the fourth mass loss step, which can be seen from Fig. 5.

The release of the mass numbers 78, 92 and 106 mainly occurred between 350 and 550 °C and is related to the fourth mass loss step, which can be seen from Fig. 6.

In addition, the most probable decomposition products with characteristic m/z values [22] are given in Table 4.

Figure 7 shows the TG results of the measurement of the sample in a temperature range from room temperature to 600 °C in a nitrogen atmosphere with a heating rate of 20 K min^{-1}.

TG depicts the relative mass change of the sample PAA/D, the mass loss rate signal as the first derivative of TG–DTG and the Gram–Schmidt trace as the overall IR intensities. Corresponding to the DTG curve, the intensities of the Gram–Schmidt trace increase as soon as a mass loss is detected. It is more or less a mirror image of the DTG curve, and this shows that the gases interact with the infrared beam as soon as they are released and transferred to the gas cell. The Gram–Schmidt signal in contrast is collected based on the individual spectra. Therefore, it is possible that the Gram–Schmidt curve contains a data point which has no corresponding spectrum with the same

Table 4 Main volatile decomposition products and the corresponding m/z ion values with relative intensity regarding the NIST Atomic Spectra Database [23]

m/z Value	Assignment	Volatile decomposition products	Temperature range of most intensive product current/°C
15	CH_3	Radical $^{*}CH_3$	150–530
16	CH_4	Methane	150–450
17	HO	Radical $^{*}OH$	150–450
18	H_2O	Water	150–450
38	C_3H_2	Cyclopropenylidene	350–550
40	C_3H_4	Cyclopropene methylacetylene	350–550
41	C_3H_5	Allyl radical	350–550
42	C_3H_6	Propene	350–550
43	C_3H_7	Radical propane	350–550
44	CO_2	Carbon dioxide	350–550
78	C_6H_6	benzene,	350–550
92	C_7H_8	toluene,	350–550
106	C_8H_{10}	ethylbenzene, o-, m-, p-xylene,	350–550

temperature. Therefore, typically the nearest temperature available spectrum is taken for evaluation of the FTIR data.

Four mass loss steps can be detected comparable to the STA results, with DTG minima at 160, 251, 315 and 418 °C. Additional peaks in the Gram–Schmidt curve are visible which are evaluated with the help of two-dimensional spectra. A residual mass of about 25% can be detected.

Accounting for the trajectories of TG–DTG and Gram–Schmidt curves (Fig. 7), gas product IR spectra were extracted for a given mass loss (Fig. 8).

In conjunction with an increase in temperature, physical and chemical changes may occur associated with the multi-stage decomposition of the PAA/D composition. The first loss of mass is related to the evaporation of the water fraction of the solvent, and the next loss is related to the evaporation of the hydration water (100–230 °C) [24, 25]. The IR spectrum obtained at a temperature of 163 °C is related to the release of water, which was confirmed by comparing this spectrum with the model IR spectrum for water (library spectrum) (Fig. 9).

During the second loss of mass at 253 °C, water is released, along with CO_2. The IR spectrum extracted at a

temperature of 253 °C (spectrum 1, Fig. 10) is presented together with the model spectra for water and CO_2 (spectra 2 and 3, Fig. 10). The presence of CO_2 which was observed is associated with the decomposition of side groups on the polymer chains.

The water arises as a result of an intermolecular dehydration reaction (Fig. 11). This dehydration process is related to the formation intermolecular anhydride cross-links between carboxyl groups of neighbouring polymer chains (chemical cross-linking) [17, 21, 26].

The third and fourth losses of mass are primarily related to the emission of CO_2, CO and low molecular weight organic compounds (Figs. 12, 14, 15). The IR spectrum extracted at a temperature of 326 °C (spectrum 1, Fig. 12) is presented together with model spectra for CO_2 (spectra 2 and 3, Fig. 12).

Above a temperature of 300 °C, fragmentation of the polyacrylic chains occurred. Additionally, side groups experience breaking of bonds in the poly(acrylic acid) chain in the carboxyl group (Fig. 13).

Within a temperature range of 400 and 464 °C, the release of methane and organic components occurs. Here,
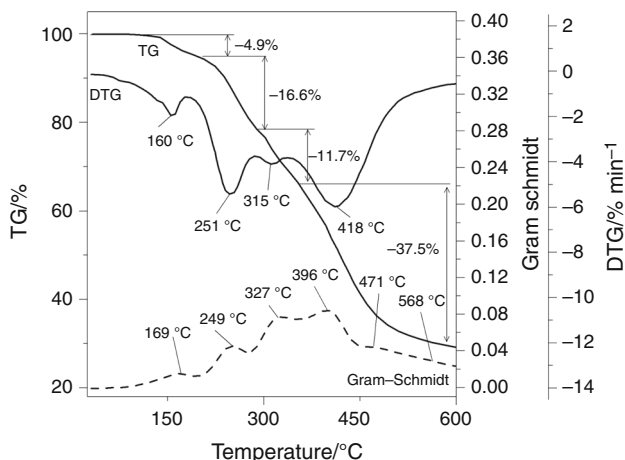
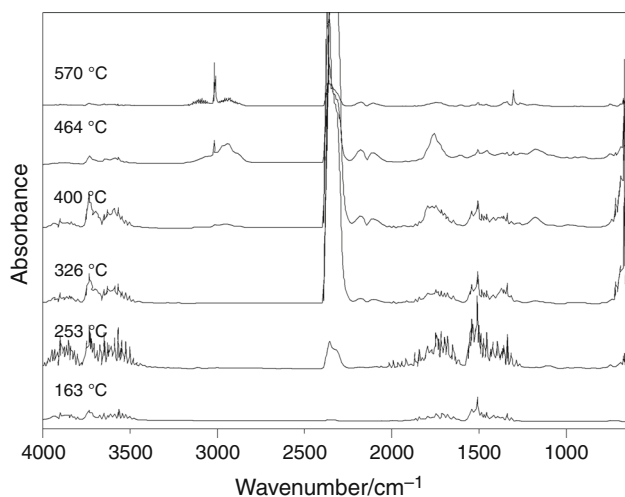Fig. 7 TG–DTG and Gram–Schmidt curves of PAA/D composition

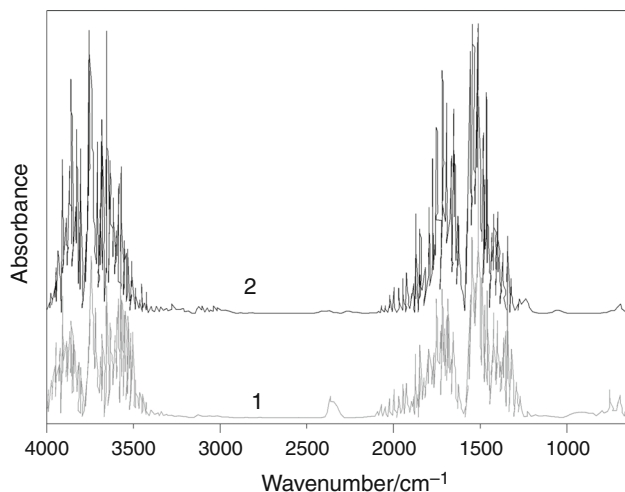Fig. 8 Extracted IR spectra of the specimen at temperature: 163, 253, 326, 400, 464 and 570 °C

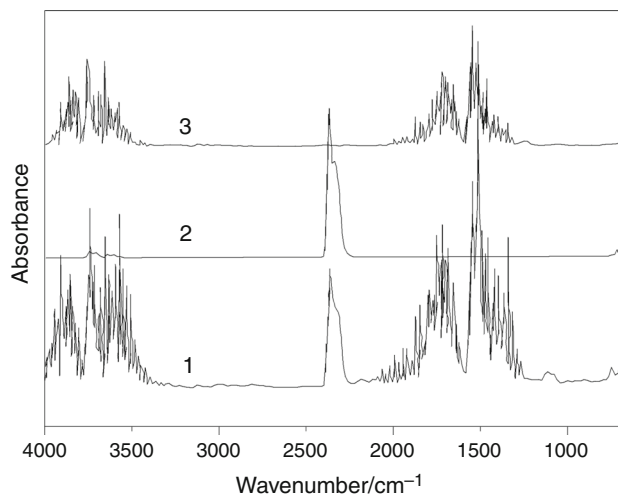Fig. 9 Comparison of the extracted IR spectrum at 163 °C (*spectrum 1*) with the library spectrum of water (*spectrum 2*)

Fig. 10 Comparison of the extracted IR spectrum at 253 °C (*spectrum 1*) with the library spectra: (2) CO_2 and (3) water
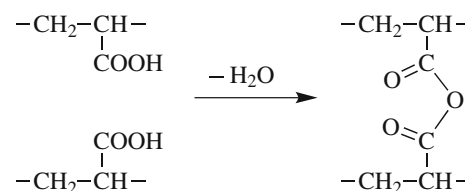

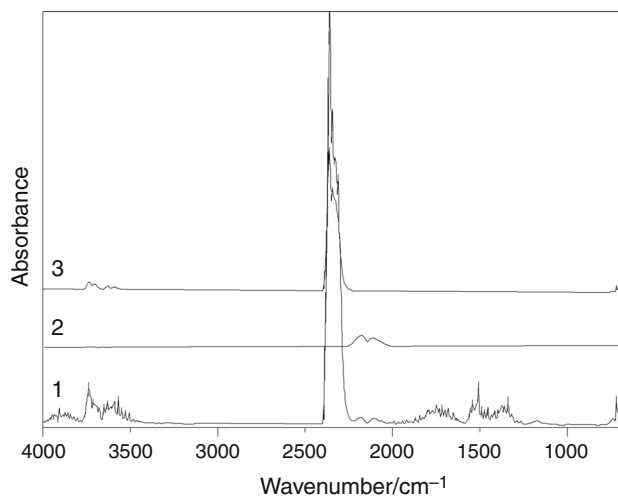
Fig. 11 Intermolecular dehydration reaction

Fig. 12 Comparison of the extracted IR spectrum at 326 °C (*spectrum 1*) with the library spectra of CO (*spectrum 2*) and CO_2 (*spectrum 3*)

as an example the IR spectrum of 3-methyl-2-cyclopenten-1-one is shown in Fig. 14. Thermal degradation of PAA/D is also associated with the decomposition of weak C–O–C bonds present in the glycosidic bond (dextrin), as well as with the formation of oligomeric radicals, which undergo further decomposition forming radicals with even shorter

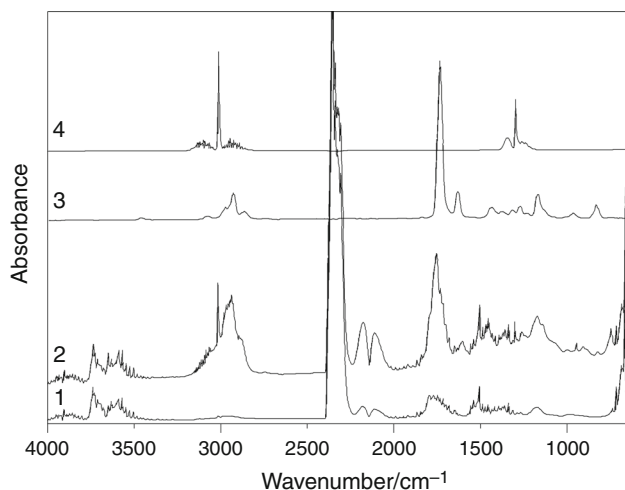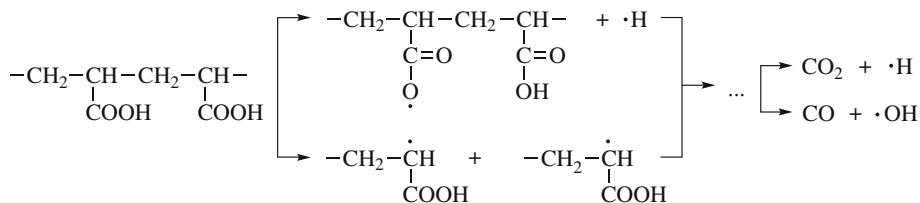Fig. 13 Diagram of degradation in the poly(acrylic acid)

Fig. 14 Comparison of the extracted IR spectrum at: 400 °C (*spectrum 1*), 464 °C (*spectrum 2*) and with the library spectra of: (3) 3-methyl-2-cyclopenten-1-one, (4) methane
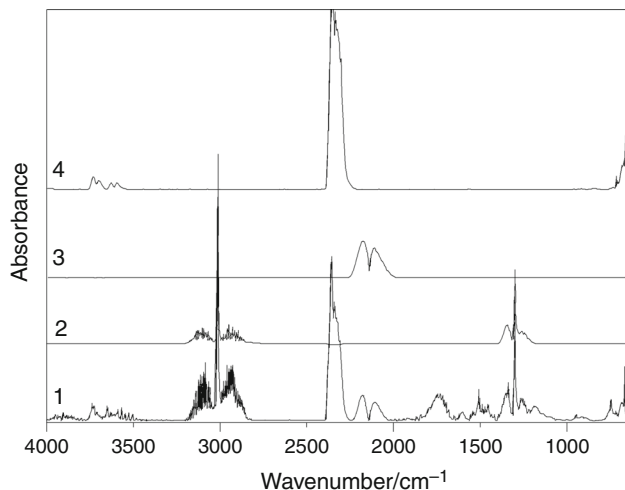

Fig. 15 Comparison of the extracted IR spectrum at 570 °C (*spectrum 1*) with the library spectra of: (2) methane, (3) CO and (4) CO_2

Conclusions

The comprehensive thermal analysis conducted in this study (TG–DSC, TG–MS, TG–IR) permits us to determine the temperatures below which PAA/D polymer compositions do not experience thermal degradation, undergoing only reversible changes, meaning that they do not lose their binding properties. The information obtained is essential in regard to the optimisation of conditions in the hardening process using conventional heating methods, and using microwave radiation in the polymer binder–matrix system, as well as in the context of the process of pouring molten metal into the mould. Moreover, the use of coupled TG–MS and TG–IR methods allows us to predict the gaseous products of the degradation of polymer compositions, an important piece of information that addresses to environmental concerns regarding the emission of gaseous substances during the casting process, i.e. at the moment of contact between the components of the hardened mould and the molten metal.

chains. For this reason, are formed cyclic ketones (3-methyl-2-cyclopenten-1-one) [18–20].

At temperature 570 °C methane, CO and CO_2 can still be detected. In Fig. 15, the IR spectrum extracted at 570 °C (spectrum 1) is presented together with the library spectra of methane, CO and CO_2 (spectra 3 and 4).

References

1. Zhou X, Yang J, Su D, Qu G. The high-temperature resistant mechanism of α-starch composite binder for foundry. J Mater Process Technol. 2009;209:5394–8.
2. Kubecki M, Holtzer M, Żymankowska S. Investigations of the Temperature Influence on Formation of Compounds from the BTEX Group During the Thermal Decomposition of Furan Resin. Arch Foundry Eng. 2013;13:85–90.
3. Grabowska B, Szucki M, Suchy JS, Eichholz S, Hodor K. Thermal degradation behavior of cellulose-based materialfor gating systems in iron casting production. Polimery/Polymers. 2013;58:39–44.
4. Wang Y, Huang H, Cannon FS, Voigt RC, Komarneni S, Furness JC. Evaluation of volatile hydrocarbon emission characteristics of carbonaceous additives in green sand foundries. Environ Sci Technol. 2007;41:2957–63.
5. Dungan RS, Kukier U, Lee B. Blending foundry sands with soil: effect on dehydrogenase activity. Sci Total Environ. 2006;357:221–30.

6. Ahamad T, Alshehri SM. Thermal degradation and evolved gas analysis of thioureaformaldehyde resin (TFR) during pyrolysis and combustion. J Therm Anal Calorim. 2012;109:1039–47.

7. Naro RL. Battling the elusive lustrous carbon defect. Mod Cast. 2003;5:32–5.

8. Chakherlou TN, Mahdinia YV, Akbari A. Influence of lustrous carbon defects on the fatigue life of ductile iron castings using lost foam process. Mater Des. 2011;32:162–9.

9. Grabowska B, Holtzer M, Dańko R, Górny M, Bobrowski A, Olejnik E. New BioCo binders containing biopolymers for foundry industry. Metalurgija. 2013;52:47–50.

10. Grabowska B, Sitarz M, Olejnik E, Kaczmarska K, Tyliszczak B. FT-IR and FT-Raman studies of cross-linking processes with Ca^{2+} ions, glutaraldehyde and microwave radiation for polymer composition of poly(acrylic acid)/sodium salt of carboxymethyl starch—In moulding sands, Part II. Spectrochim Acta Part A Mol Biomol Spectrosc. 2015;151:27–33.

11. Grabowska B, Sitarz M, Olejnik E, Kaczmarska K. FT-IR and FT-Raman studies of cross-linking processes with Ca2 + ions, glutaraldehyde and microwave radiation for polymer composition of poly(acrylic acid)/sodium salt of carboxymethyl starch—Part I. Spectrochim Acta Part A Mol Biomol Spectrosc. 2015;135:529–35.

12. Fox JT, Cannon FS, Brown NR, Huang H, Furness JC. Comparison of a new, green foundry binder with conventional foundry binders. Int J Adhes Adhes. 2012;34:38–45.

13. Grabowska B, Malinowski P, Szucki M, Byczyński Ł. Thermal analysis in foundry technology. J Therm Anal Calorim. 2016;126:245–50.

14. Pielichowski J, Pielichowski K. Application of thermal analysis for the investigation of polymer degradation processes. J Therm Anal. 1995;43:505–8.

15. Jelínek P, Buchtele J, Fiala J. Forms of pyrolytic carbon ensuing on thermal degradation of coal and carbonaceous additives. Acta Metall Slovaca. 1999;5:112–8.

16. Zhang H, Zhao H, Zheng K, Li X, Liu G, Wang Y. Diminishing hazardous air pollutant emissions from pyrolysis of furan no-bake binders using methanesulfonic acid as the binder catalyst. J Therm Anal Calorim. 2014;116:373–81.

17. Lattimer RP. Pyrolysis mass spectrometry of acrylic acid polymers. J Anal Appl Pyrolysis. 2003;68–69:3–14.

18. Lluch AV, Felipe AM, Greus AR, Cadenato A, Ramis X, Salla JM, et al. Thermal analysis characterization of the degradation of biodegradable starch blends in soil. J Appl Polym Sci. 2005;96:358–71.

19. Lawal OS, Lechner MD, Kulicke WM. The synthesis conditions, characterizations and thermal degradation studies of an etherified starch from an unconventional source. Polym Degrad Stab. 2008;93:1520–8.

20. Tudorachi N, Lipsa R, Mustata FR. Thermal Degradation of Carboxymethyl Starch -g-Poly (lactic acid) Copolymer by TG–FTIR–MS Analysis. Ind Eng Chem Res. 2012;51:15537–45.

21. McNeill IC, Sadeghi SMT. Thermal stability and degradation mechanisms of poly(acrylic acid) and its salts: part 1—Poly(acrylic acid). Polym Degrad Stab. 1990;29:233–46.

22. Dubinsky S, Grader GS, Shter GE, Silverstein MS. Thermal degradation of poly(acrylic acid) containing copper nitrate. Polym Degrad Stab. 2004;86:171–8.

23. NIST chemistry webbook standard reference database number 69. 2011. http://webbook.nist.gov/chemistry.

24. Bednarek P, Szafran M. Thermal decomposition of monosaccharides derivatives applied in ceramic gelcasting process investigated by the coupled DTA/TG/MS analysis. J Therm Anal Calorim. 2012;109:773–82.

25. Šimkovic I, Jakab E. Thermogravimetry/mass spectrometry study of weakly basic starch-based ion exchanger. Carbohydr Polym. 2001;45:53–9.

26. Greenberg AR, Kamel I. Kinetics of anhydride formation in poly(acrylic acid) and its effect on the properties of a PAA-alumina composite. J Polym Sci Polym Chem Ed. 1977;15:2137–49.